Distinction between Hydration and Fertigation Events in Plant Tetrapolar Bioimpedance Measurements

Enayetur Rahman
School of Sci. and Tech. (SST)
City, Univ. of London
London, UK
enayet.rahman.2@city...

Bojan Nikolic
SST
City, Univ. of London
London, UK
bojan.nikolic.2@city...

Michael Powner
School of Health & Psy. Sci.
City, Univ. of London
London, UK
michael.powner@city...

Panos Ioakim
Delta-T Devices Ltd
Cambridge, UK

Iasonas F. Triantis
SST
City, Univ. of London
London, UK
i.triantis@city.ac.uk

***Abstract*—In this study, we assess the appropriateness of tetrapolar bioimpedance needle plant sensors for interrogating the full plant stem and for differentiating between hydration (watering) and fertigation (feeding) events in herbaceous plants. Our sensor features a tetrapolar configuration of needle electrodes arranged in "paired pairs". The goal is to develop a bioimpedance-based sensor that automatically monitors watering and fertigation status in tomato plants, offering optimal performance, easy installation, and cost-effectiveness. We detail our design methodology using COMSOL FEM simulations to assess the needle geometry in terms of its ability to effectively interrogate the stem across its diameter. The tomato stem's bioimpedance was modelled as a lumped-impedance equivalent circuit, with R and C values computed from experimental data. The theoretical model indicated similar characteristics to those extracted experimentally. Experiments were carried out over 27 days with impedance magnitude and phase periodically monitored for ten frequencies, with the results clearly indicating watering and feeding events, which were accurately classified using a PCA-based clustering algorithm.**

***Index Terms*—plant sensor, plant wearable, bioimpedance, impedance, tetrapolar, cuff electrode, cable-tie cuff, flexible PCB.**

I. Introduction

Monitoring watering and feeding events in plants is critical for optimizing agricultural practices and ensuring sustainable crop production. Traditional soil sensing methods, while useful, often fail to provide detailed insights into the plant's immediate physiological responses. Direct on-plant sensing, especially when applied to specific structures like the stem, offers a more detailed and comprehensive understanding of plant health and resource utilization [1]–[3]. This method allows for real-time monitoring of plant conditions, which is crucial for making timely and informed decisions about watering and fertilization.

On-plant sensors are particularly significant as they directly measure the plant's physiological status, offering insights that are not possible through soil sensing alone. By measuring parameters such as moisture levels and nutrient uptake directly from the plant, these sensors can help understand how plants respond to environmental conditions and management practices. This information is invaluable for precision agriculture, where accurate and timely data can improve crop yields and resource efficiency.

In this study, we focus on using tetrapolar needle electrodes for monitoring physiological changes in the tomato plant (Solanum lycopersicum) stem. This method builds on our previous work, where we introduced a novel tomato plant "wearable" bioimpedance sensor based on cuff electrodes [4]. Needle electrodes, offer better spatial resolution compared to other on-plant solutions, allowing for more precise measurements at specific locations within the stem [1], [2]. This increased spatial resolution is essential for capturing localized variations in plant tissue, providing a more granular understanding of plant health and stress responses. Whilst previous work [2] has demonstrated the appropriateness of needle electrodes for monitoring hydration related events in plants, their appropriateness for fertigation monitoring and especially for the distinction between feeding and watering events has not been demonstrated. Moreover, the portion of the plant stem cross sectional area being interrogated by needle electrodes was not assessed and therefore the electrode topology has not been previously designed through a systematic procedure. Tetrapolar electrodes present a significant improvement over the more commonly used bipolar electrodes [5]. The primary advantage lies in their ability to minimize the impact of electrode polarisation and contact impedance, leading to more accurate and reliable measurements of the plant's electrical properties. This is particularly important in the context of monitoring dynamic events such as changes in moisture levels and nutrient uptake, which are directly influenced by watering and feeding practices. However, tetrapolar electrode configurations also suffer setbacks, including geometry-related negative sensitivity regions that may give rise to errors and non-linearities necessitating a systematic approach to their design. To optimize the design and deployment of tetrapolar needle electrodes in plants, this paper presents COMSOL FEM simulations, taking into account the electrical properties of the tomato stem. These simulations were used to determine

Royal Academy of Engineering Industrial Fellowship IF2324-A162.

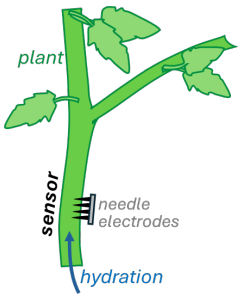

Fig. 1: Conceptual representation of wearable bioimpedance sensors.

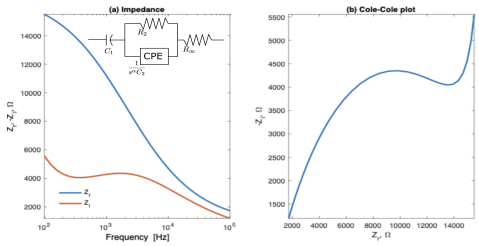

Fig. 2: Impedance and Cole-Cole diagram

the optimal sensor geometry for accurate data acquisition. We then carried out experiments in a controlled environment. Our experimental setup involved embedding the needle electrodes into the tomato stem and monitoring the plant under varying conditions of moisture and nutrient presence.

The results from our initial experiments demonstrate that tetrapolar needle electrodes can effectively capture real-time data reflecting the plant's physiological status. The data is then analyzed using unsupervised machine learning algorithms, specifically Principal Component Analysis (PCA) [6], to identify hidden variables that aid in data classification. A Support Vector Machine (SVM) [7] based linear classifier was used for the classification. A simple model using electrical components was also developed with the parameters calculated from the experimental data. This data and the model are essential for developing more precise and responsive irrigation and fertilization strategies, ultimately promoting resource-efficient and sustainable agricultural practices.

II. Materials and Methods

In this study, we aimed to investigate the use of tetrapolar need electrodes inserted into a plant stem (tomato) for impedance measurements. Over a period of two weeks, we conducted several watering and feeding events while recording the tetrapolar transfer impedance with one continuous measurement every 22 minutes. The magnitude and phase of the measured transfer impedance were recorded using a standard impedance analyzer.

As part of our methodology, we developed a simple model in COMSOL. This model consisted of a cylinder representing the tomato stem with an effective material property (permittivity and conductivity). The purpose of this model was to provide us with an estimate of the transfer impedance we could expect from a tomato stem based on its material properties. Our model demonstrated that the measured transfer impedance is sensitive to changes in the stem's conductivity and permittivity. This suggests that we can detect conductivity variations from a measured change in transfer impedance, which could have significant implications for the concentration of ions and water in the plant.

Transfer impedance, a key component of our study, comprises conductivity and permittivity. To better understand and model this impedance, we have employed a lumped parameter electrical circuit equivalent model. This model uses a parallel combination of a resistor (R_2) and a constant phase element (CPE, $1/(j\omega)^{\alpha}C_2$) and a resistor in series (R_∞), with R_2 representing the conductive element, the CPE representing the system's permittivity and R_∞ is the resistance at extremely high frequency. Here, the parameter α has a value between 0 and 1, where $\alpha = 1$ represents pure capacitance, and for most biological materials, the value lies between $0.5 - 0.9$. An increase in conductivity decreases the resistance, and the capacitance increases with an increased permittivity. As the base medium for a plant in water, the low-frequency relative permittivity is considered 80, and the base level of conductivity is regarded as 0.1 S/m [8]. A stem of a length of 8 mm and a diameter of 4 mm can have a base resistance of 6.37 kOhm. Impedance measurements from the side using needle electrodes, however, produce a larger resistance value, which was confirmed through the Comsol simulation. The measured transfer impedance from the needle electrodes is directly proportional to the total cylindrical impedance measured from the two electrodes placed on the opposite side of the cylinder. This indicates that the transfer impedance measured is a reliable representation of the actual impedance value and can be used as a valid method for plant conductivity measurements and it can be used to monitor plant's watering and fertigation status.

When we have a capacitance from the contacts and stem impedance are considered in series, the modified circuit can be modeled as a series capacitance (C_1) and $R_2||CPE + R_\infty$ the combined stem resistance and stem capacitance. The equivalent electrical circuit is depicted in fig. 2a. The real and the imaginary impedance are given by,

$$Z_r = R_\infty + R_2 \frac{1 + \omega^{\alpha} RC \cos\frac{\alpha\pi}{2}}{1 + 2\omega^{\alpha} RC \cos\frac{\alpha\pi}{2} + (\omega^{\alpha} R_2 C_2)^2} \quad (1)$$

and,

$$|Z_i| = R_2 \frac{\omega^{\alpha} RC \sin\frac{\alpha\pi}{2}}{1 + 2\omega^{\alpha} RC \cos\frac{\alpha\pi}{2} + (\omega^{\alpha} R_2 C_2)^2} + \frac{1}{\omega C_1} \quad (2)$$

When $\omega \to 0$, $Z_i \to \infty$, therefore, the asymptote at the right side of fig. 2b is located at R_2. At $Z_r = R_2/2$, the $|Z_i| = R_2/2 \tan\frac{\alpha\pi}{4}$, using which the value for α can be determined. The frequency at which the $|Z_i|$ has a local peak is,

$$\omega_\tau = \frac{1}{(R_2 C_2)^{1/\alpha}}, \; where, \; \tau = (R_2 C_2)^{1/\alpha}$$

R_∞ can be found from Z_r at very high frequency and C_1 can be calculated from any $|Z_i|$ value from the very low-frequency

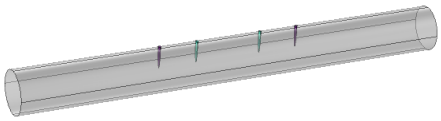

Fig. 3: Electrode configurations for tetrapolar needle electrode.

region (where the parallel RC combination has minimal effect) of Z_i by,

$$C_1 = \frac{1}{\omega |Z_i|}$$

Following the procedures described, we can determine the values for R_2, C_2, α, R_∞ and C_1 from the experimental data.

A. FEM simulations

An idealized digital twin of the plant stem, modeled as a cylinder, was created using the AC/DC module of COMSOL 5.5 (Fig. 3). This model was assigned a conductivity of 0.1 S/m and a permittivity of 80, based on [8]. The cylinder had a length of 40 mm and a diameter ranging from 2 to 5 mm. Gold (Au) was selected as the material for the needle electrodes inserted into the cylinder (Fig. 3). Different electrode-to-electrode distances and spacings between electrode pairs were simulated to identify the optimal parameters. The needle electrodes, measuring .25 mm in diameter at their broader end and 2 mm in length, penetrated the stem by 1-2 mm. In this in-line tetrapolar configuration, the two outer electrodes function as CC (current-carrying) for current injection, while the inner pair of electrodes serve as the PU (pick-up) electrodes utilized for voltage measurement. The injection current was $100\mu A$ with an insulation boundary condition. An *'extremely fine'* mesh was employed for the simulation. In the Frequency Domain study, we utilized Sensitivity distribution, S, a commonly employed parameter for tetrapolar impedance measurement systems, which is

$$S = \frac{\overline{J}_{CC} \cdot \overline{J}_{PU}}{I^2} \tag{3}$$

where $\overline{J}_{CC}$ represents the current density (A/m^2) resulting from the injected current through the CC electrodes, $\overline{J}_{PU}$ represents the current density when the currents are injected through the PU electrodes, and I is the magnitude of the applied current. The sensitivity distribution at the cross-section of the cylinder as shown in fig. 4b shows the measured impedance should have higher contributions from the neighbouring regions of the needle electrodes. The transfer impedance was calculated by

$$Z_t = \frac{V_{PU}}{I}\ \Omega \tag{4}$$

Here, V_{PU} is the potential measured between the PU electrodes when an injection current of I is applied through the CC electrodes.

B. Needle Electrode Fabrication

The needle electrodes, consisted of four gold PA2BX "spear point" Coda pins (originally spring-loaded, here springs disabled) with a maximum diameter of 0.53 mm, connected to RA2S 1.32mm ext. diameter receptacles housed in a robust plastic casing. This ensured their parallel placement and kept their tips in line. They were arranged in two pairs, each with an edge-edge inter-electrode distance of 2.54mm and an inter-pair distance of 5.08mm. Fortified with epoxy, the casing was used to exert pressure for piercing the stem, aligning the electrodes parallel to the stem axis. The electrodes were then securely fastened on the stem with several loops of soft nylon thread. Recordings were started 2 weeks post insertion to allow for stem healing.

TABLE I: Electrical equivalent circuit parameters from experimental data

Parameters	Baseline	Watering	Fertigation
C_1	$418 \pm 14\ nF$	$430 \pm 13\ nF$	$560 \pm 48\ nF$
C_2	$211.48 \pm 2\ nF$	$334.01 \pm 3\ nF$	$269.62 \pm 4\ nF$
R_2	$16458 \pm 120\ \Omega$	$17216 \pm 114\ \Omega$	$12883 \pm 220\ \Omega$
α	0.5952 ± 0.02	0.5424 ± 0.03	0.5722 ± 0.02
R_∞	$693 \pm 5\ \Omega$	$685 \pm 7\ \Omega$	$691 \pm 5\ \Omega$

C. Experimental Protocol

For our measurements, we used the Instek LCR-6100 LCR Meter [9], a versatile impedance analyzer with frequency ranges from 10 Hz to 100 kHz. This device offers a basic accuracy of 0.05 % and can measure within 25ms, ensuring rapid and reliable data acquisition. A set of impedance magnitude and phase measurements was logged to a PC every 20 minutes for 22 days. Each set comprised measurements at ten different frequencies in 5s intervals, with values of 100, 215 and 464Hz multiplied by 1, 10 and 100, and a reading at 100kHz. The plants were grown in cubes of Rockwool [10] to better control nutrient levels and to allow for better survivability in a sparse watering regime that allowed for watering and feeding events to be distinct from daily physiological variations. Locating the plants in an enclosure allowed for the control of temperature (19°C), humidity (65-75%), CO_2 (650-950 ppm) and light (between 8am and 6pm daily, provided by a 1000W full spectrum grow light).

III. Results

The magnitude and phase data indicate that watering and fertigation events significantly influence the measured impedance magnitude and phase (Figure 6). The real (Z_r) and imaginary (Z_i) components of the impedance, derived from the experimental values of $|Z|$ and ϕ, are calculated using the equations $Z_r = |Z|\cos(\phi)$ and $Z_i = |Z|\sin(\phi)$, respectively. All Z_r and Z_i values exhibit similar shapes, with variations in magnitude and peak locations in $|Z_i|$ (Figure 5a). The Cole-Cole plots reveal distinct differences in the height, width, and location of ω_τ among watering, fertigation, and equilibrium states of the stem (Figure 5b). From Figure 5b it can be observed from the Cole-Cole plots that watering and fertigation events change the shape of the curves significantly. Table I is showing the calculated values for R_∞, R_2, C_2, α and C_1, along with their standard deviations, derived from the experimental data. After watering or fertigation, changes

in R_∞, R_2, C_2, and C_1 are observed. It has been found that R_∞ remains unchanged at around 690 Ω. R_2 value, which represents the resistance of the stem is increased after an watering event by 3.5%, the C_2 value, which represents the effective permittivity value of the stem is reduced by about 3.5%, however the α reduces by 5%. These results indicate the effective permittivty decreases after watering event and the effective conductivity reduces due to the dilution of the ions in the stem. The fertigation event decreases the R_2 value significantly (by about 25%) that indicates an increased concentration of ions in the stem. The C_2 value is decreased by 9% indicates that the effective permittivity is reduced that is a combined effect of additinal water and ions in the stem after fertigation. The fertigation reduces the α from its baseline value by 4%. From fig. 6 we can observe a periodic daily variations in the base impedance level, which can be the effects of the variation of light levels and other activities during the day and at night within the plant.

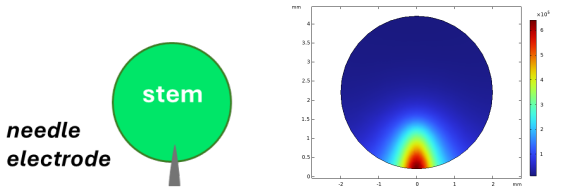

(a) Needle cross-section (b) Needle Sensitivity

Fig. 4: Sensitivity distribution cross section

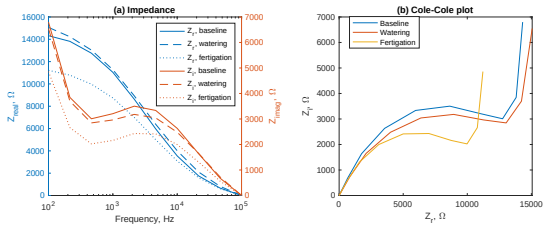

Fig. 5: Effects of watering and fertigation on impedance and Cole-Cole plot

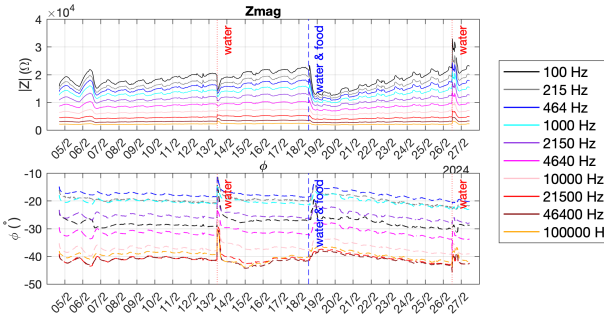

Fig. 6: Effects of watering and fertigation on Time plot

Principal Component Analysis (PCA) is a statistical technique for dimensionality reduction, data compression, and feature extraction. It transforms correlated variables into uncorrelated principal components. A PCA score plot visually represents data in the principal component space, aiding in the classification and understanding of the data's underlying structure by displaying the principal component scores. In the plot, the x-axis represents the first principal component, which captures the most variance in the data, while the y-axis represents the second principal component, which captures the second most variance. Figure 7 shows the PCA score plot on a dataset containing three classes of data, 'Baseline', 'Watering' and 'Fertigation'. The PCA score plot shows that the data from different classes are clustered. The clustering indicates that developing a classification algorithm to classify and detect various events from the captured impedance data is possible. A Support Vector Machine (SVM) based linear classifier produced a classification accuracy of 99.3%.

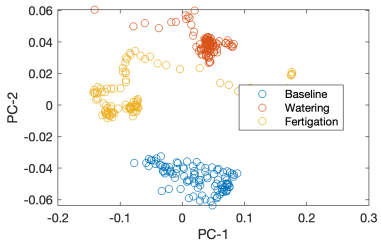

Fig. 7: Principal component analysis for classifying baseline, watering and fertigation events

IV. Conclusions

In conclusion, our study presents a bioimpedance needle sensor designed for tomato plants to monitor watering and fertigation events. This sensor employs an asymmetric tetrapolar needle electrode configuration optimized to detect changes in bioimpedance associated with hydration and fertigation. The primary objective was to create a sensor that automatically monitors watering and fertigation status and ensures optimal performance, ease of installation, durability, and cost-effectiveness. Our comprehensive design methodology utilized COMSOL FEM simulations to fine-tune the needle geometry, ensuring maximum sensitivity and accuracy. We modeled the tomato stem's bioimpedance using an electrical circuit equivalent, incorporating a series capacitor and a parallel combination of a resistor and another capacitor. The R and C values, crucial for accurate modeling, were derived from experimental data. This model aligns closely with experimental measurements, demonstrating a high level of accuracy. Collecting further data in a more controlled environment could lead to an even more precise model. Furthermore, we employed a PCA-based clustering algorithm to analyze the sensor data, which successfully classified the watering and fertigation events accurately. This capability highlights the potential of our sensor to significantly enhance automated irrigation systems by providing precise and real-time monitoring of plant hydration and fertigation status. Our findings pave the way for advanced agricultural practices, offering a robust tool for optimizing water and nutrient delivery, ultimately contributing to more efficient and sustainable farming.

ACKNOWLEDGMENT

This work is supported by Royal Academy of Engineering Industrial Fellowship IF2324-A162 granted to Dr I. F. Triantis for the development of plant wearable biosensors in collaboration with Delta-T Devices Ltd.

REFERENCES

[1] G. Dufil, I. Bernacka-Wojcik, A. Armada-Moreira, and E. Stavrinidou, "Plant bioelectronics and biohybrids: the growing contribution of organic electronic and carbon-based materials," *Chemical Reviews*, vol. 122, no. 4, pp. 4847–4883, 2021.

[2] L. Bar-On and Y. Shacham-Diamand, "On the interpretation of four point impedance spectroscopy of plant dehydration monitoring," *IEEE Journal on Emerging and Selected Topics in Circuits and Systems*, vol. 11, no. 3, pp. 482–492, 2021.

[3] R. Chen, S. Ren, S. Li, D. Han, K. Qin, X. Jia, H. Zhou, and Z. Gao, "Recent advances and prospects in wearable plant sensors," *Reviews in Environmental Science and Bio/Technology*, vol. 22, 08 2023.

[4] E. Rahman, B. Nikolic, M. Freeman, S. Goralik, P. Ioakim, and I. Triantis, "Design of a cuff electrode - inspired wearable bioimpedance plant sensor," *IEEE BioSensors 2024. Accepted for presentation*, 2024.

[5] P. Bertemes-Filho and K. F. Morcelles, *Wearable Bioimpedance Measuring Devices*. Cham: Springer International Publishing, 2022, pp. 81–101.

[6] M. Greenacre, P. J. Groenen, T. Hastie, A. I. d'Enza, A. Markos, and E. Tuzhilina, "Principal component analysis," *Nature Reviews Methods Primers*, vol. 2, no. 1, p. 100, 2022.

[7] D. A. Pisner and D. M. Schnyer, "Support vector machine," in *Machine learning*. Elsevier, 2020, pp. 101–121.

[8] I. Bodale, G. Mihalache, V. Achiţei, G.-C. Teliban, A. Cazacu, and V. Stoleru, "Evaluation of the nutrients uptake by tomato plants in different phenological stages using an electrical conductivity technique," *Agriculture*, vol. 11, no. 4, p. 292, 2021.

[9] Gwinstek. Technical specification. [Online]. Available: https://www.gwinstek.com/en-US/products/detail/LCR-6000

[10] C. Sonneveld, "Rockwool as a substrate for greenhouse crops," in *High-Tech and Micropropagation I*. Springer, 1991, pp. 285–312.